EasyChair Preprint

№ 1843

Use of Electrical Energy Storage to Improve the Voltage Stability of a Power System with Large Amount of Wind Generation

Ziphezinhle Kazi, Kehinde Awodele, Bongane Nhlapo and Victor Adebayo

November 5, 2019

Use of Electrical Energy Storage to Improve the Voltage Stability of a Power System with Large Amount of Wind Generation

Ziphezinhle N. Kazi
Dept. of Electrical Engineering
University of Cape Town
Cape Town, South Africa
KZXZIP001@myuct.ac.za

Kehinde O. Awodele, MIEEE
Dept. of Electrical Engineering
University of Cape Town
Cape Town, South Africa
kehinde.awodele@uct.ac.za

Bongane Nhlapo
Transmission Grid Planning
Eskom
Sunninghill, South Africa
NhlapoJB@eskom.co.za

Adebayo A.V.
Dept. of Electrical Engineering
University of Cape Town
Cape Town, South Africa
victor.adebayo@alumni.uct.ac.za

***Abstract*—This paper proposes the use of the Energy Storage System (BESS) to improve the voltage stability on a small-scale South African network with a large amount of wind power generation; under both steady-state and fault conditions. Pumped-Hydroelectric Storage (PHS) and BESS were selected and compared in DIgSILENT PowerFactory 2018 simulation software. Mathematical models and block models of the network components, BESS and PHS models were developed and tested under steady-state operation, thus, three cases were studied which included the network with wind power generation, then with wind power generation and BESS and finally with wind power generation and PHS.**

Results under steady-state conditions showed that the voltage levels for the four loads were within the acceptable standard voltage limits of 0.95 p.u. and 1.05 p.u. across all three cases. Thus, it was concluded that BESS is the most suitable EES for a network with a large amount of wind generation, as it displayed the capability of maintaining the voltage levels within the acceptable voltage limits under both steady-state and fault conditions.

Keywords— Electrical energy storage; battery energy storage system; pumped-hydroelectric storage; three-phase fault; voltage stability.

I. INTRODUCTION

In the past, electricity generation in South Africa has been mainly from coal and nuclear energy sources with hydropower being largely imported from the neighboring countries [1]. However, the result of deteriorating ecosystems, increased depletion of coal, negative contribution of burning coal towards the environment and climate change; has led to widespread calls for changes to the country's energy mix. This has led to renewable energy sources such as wind energy to be considered in the energy mix. Hence, the drafted South African Integrated Resource Plan (IRP) 2018 seeks to map out a future that will fully accommodate the integration of renewable energy into the grid [1]. The integration of renewable energy sources into the grid poses some challenges, as these sources are sporadic and do not produce a constant supply of electricity like fossil fuels [1]. This is a result of renewables being weather-dependent. The location-dependent and sporadic nature of wind turbine generators can result in, power quality problems such as voltage dips, flicker, harmonics, frequency variations and low power factor [2].

Introducing wind power generators will have a positive environmental impact as it will reduce the emissions of greenhouse gases. The use of electrical energy storage (EES) is expected to make it easier to integrate wind turbines generators into the power system. Pumped Hydroelectric Storage (PHS) is the most popular form of EES currently deployed in South Africa for peak-levelling applications; while Battery Energy Storage System (BESS) is the most promising EES which is used in small-scale and large-scale power systems across the world [3]. Hence, investigating the ability of both BESS and PHS to improve the voltage levels of the network with wind power generation under both steady-state, and fault conditions will be extremely beneficial. The network that will be studied is a small-scale South African network in the Eastern Cape Province with a large amount of wind generation. Therefore, this investigation will assist in proposing which EES between BESS and PHS will best improve the voltage stability of a small-scale network with a large amount of wind generation.

A small-scale network was developed, which consists of several busbars, seven Open-cycle Gas Turbine (OCGT) generators, three substations, 14 wind farms which are connected at two substations, three external grids which represent the upstream networks, and several transformers and transmission lines interconnecting the respective buses as shown in Fig. 1:

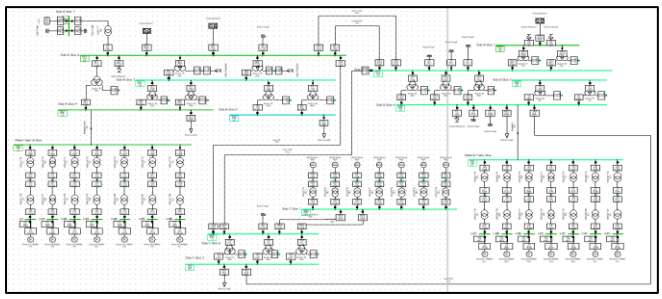

Fig. 1: Selected Power System Network

The selected network is a small-scale South African network located in the Eastern Cape, with large amount of wind generation. The wind farms add generation capacity to the small-scale grid originally importing power from the upstream

network and also powered by open cycle gas turbine (OCGT) generators during peak load conditions. The seven wind power generators connected at Substation A have a total output of 848 MW, while the other seven generators connected at Substation B have a total output of 649 MW. The individual components of the power system network in Fig. 1 were modelled in DIgSILENT PowerFactory.

II. Battery Energy Storage System Modelling

The most prominent BESS used in industry are often lead-acid and lithium-ion batteries [3]. Different approaches to modelling lead-acid based BESS models are reviewed and documented in [4] and [5]. For this research, the simple equivalent circuits shown in Fig. 2 are used to model the required battery model.

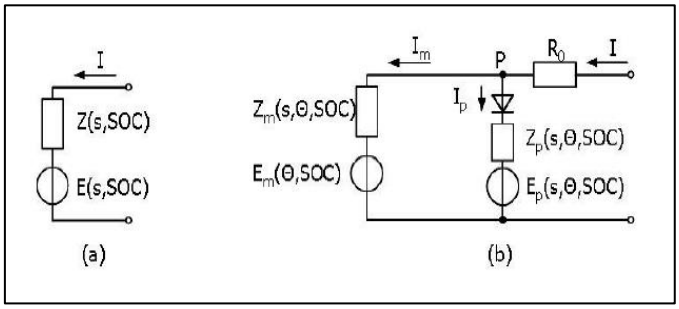

Fig. 2: Battery Electric Equivalent, (a) Simple, (b) with Parasitic Reaction *[5]*

Referring to Fig. 2, BESS can be modelled using the capacity of the BESS and the most appropriate equation to relate the capacity of the battery with time is known as Peukert's Law (1) [6]. Peukert's Law helps to relate the battery's capacity in terms of the rate at which the battery discharges. This means that the battery's capacity decreases as the rate of discharge increases [6]. This theory is mathematically illustrated by the following equation [6]:

$$C_p = I^k t \quad (1)$$

Where:
C_p is the capacity of the battery at a one-ampere (1A) discharge rate and is expressed in Ah.
I is the discharge current in ampere (A).
k is the Peukert constant.
t is the time of discharge in hours (h).

The capacity of the battery is assumed to be constant in order to simplify the calculations. This assumption is made in the case where the discharge current is known as shown in (1); that the capacity is dependent on the discharging current.

The battery model is implemented on Dynamic Simulation Language (DSL) as shown in Fig. 3:

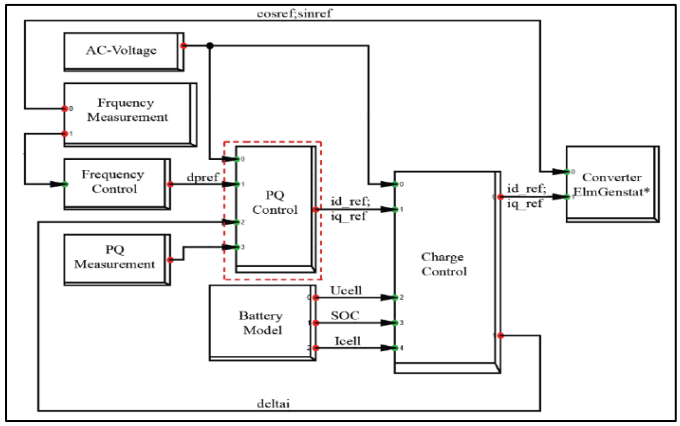

Fig. 3: Framework of BESS Controller Available in DIgSILENT *[5]*

Referring to Fig. 3, the BESS model consists of frequency, PQ and charge control blocks, and the converter block. The BESS model available in DIgSILENT consists of the three major components, which are required to control the BESS performance and they are described as follows:

A. Frequency Control

The frequency block in Fig. 3 controls frequency support which allows the BESS to supply and absorb real power during frequency trips. This operation is performed by comparing the system frequency to the nominal value. Thus, when there is a mismatch detected, a signal is sent to the BESS to inject more power in the event that the measured frequency is more than 2 Hz below the nominal value of 50 Hz. While in the event that the frequency is greater than 2 Hz above the nominal value, the BESS will absorb power from the grid [6], [8].

PQ Control

The PQ-control block is connected to the frequency block. The PQ-controller controls and regulates the active and reactive power and the bus voltage using the PI-controller method [6], [8].

Charge Control

The charge controller is connected to the PQ-control block and the battery model as shown in Fig. 3. The charge control block will send a signal to the BESS to absorb active power from the PQ-controller depending on the State of Charge (SOC) of the battery and nominal frequency [8]. The charge control is modelled such that the SOC of the BESS model is limited between zero and one. When SOC is equal to one, the BESS is fully charged. Hence, active power can no longer be absorbed by the BESS.

Voltage Source Converter Modelling

The majority of battery storage systems are DC voltage sources. Thus, AC-DC or DC-AC converters are required to convert DC-voltage to AC-voltage and vice versa. For this research, the Pulse Width Modulation (PWM) converter is used to convert the DC-voltage from the battery source to an AC-voltage since the network is operating at AC voltage. The PWM converters are usually referred to as Voltage Source Converter (VSC),

which convert DC-voltage into AC-voltage through fast switching of IGBT-valves [6]. The switching signal also known as the amplification factor (P m) arrives from the control system of the VSC and the model for frequency of the PWM can be expressed by using the following equations [6]:

$$U_{AC_r} = K_0 P_{m_r} U_{DC} \quad (2)$$

$$U_{AC_i} = K_0 P_{m_i} U_{DC} \quad (3)$$

Where:
U_{AC_r} is the real part of the AC-voltage measured in volts (V).
U_{AC_i} is the imaginary part of the AC-voltage measured in volts (V).
U_{DC} is the DC-voltage of the battery measured in volts (V).
K_0 is the constant factor which depends on the PWM-method used.

For the sinusoidal PWM-method it is given by the following expression [6]:

$$K_0 = \frac{\sqrt{3}}{2\sqrt{3}} \quad (4)$$

Assuming that the converter is lossless, the converter can be characterized using (5) which relates the power conservation between the AC and DC voltages:

$$P_{AC} = \mathbb{R}(U_{AC} {I_{AC}}^*) = U_{DC} I_{DC} = P_{DC} \quad (5)$$

The PWM converter is modelled in such a way that it operates under 0.9 kV and 0.4 kV line-to-line nominal voltages. The AC-side of the PWM is connected to the AC bus with a nominal voltage of 0.4 kV and then connected to the step-up transformer. The DC-side of the PWM is connected to the battery via a DC bus with a nominal voltage of 0.9 kV. The PWM converter is rated at 30 MVA and the converter type is modelled as a two-level converter. The method of modulation is sinusoidal PWM with the modulation constant K_o as explained above.

III. Pumped-Hydroelectric Plant Modelling

Considering the hydroelectric generation system shown in Fig. 4:

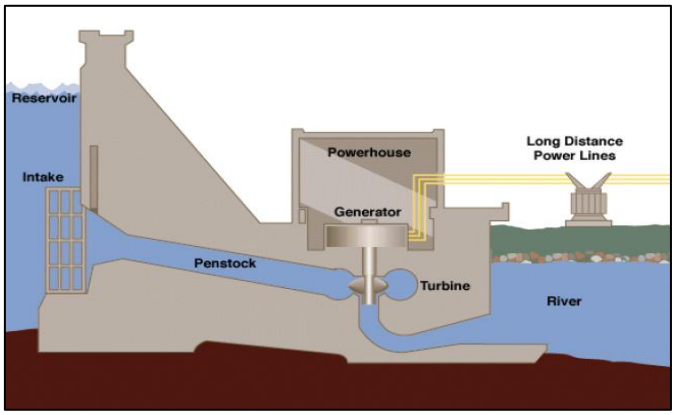

Fig. 4: Hydroelectric Dam, Turbine, and Generator *[6]*

The amount of water flowing into the penstock is controlled by a control gate at the intake. The water in the penstock flows through the turbine and rotates it, prior to being discharged through the draft tube. The turbine is coupled to a synchronous generator, which is connected to the electrical network. The gate position is controlled by a governor system, which attempts to keep the output of the generator at a constant frequency. A voltage controller is also connected to the generator, controlling the terminal voltage of the machine by regulating the rotor excitation [9].

Referring to Fig. 4 there are control signals (i.e. gate position, excitation voltage), control objectives and feedback (i.e. frequency, terminal voltage). Hence, this can be reduced and characterized by a block diagram as shown in Fig. 5:

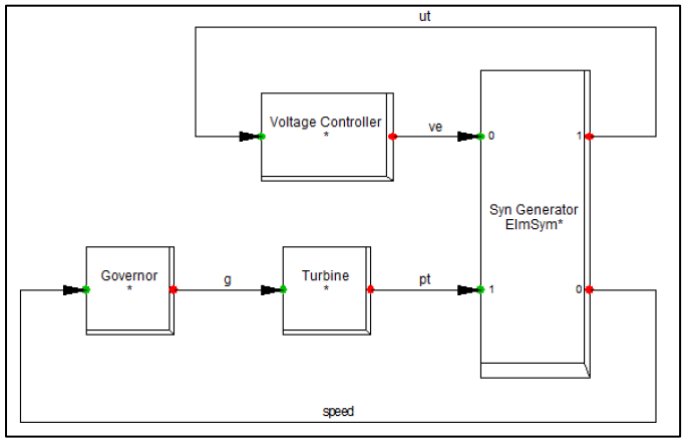

Fig. 5: Composite Frame for Hydroelectric Generation System *[6]*

The block diagram in Fig. 5 represents the composite frame for the hydroelectric system. It shows how the synchronous generator, governor, turbine and voltage controller are connected and the input/output signals between them. There is already a built-in model for the synchronous generator element and therefore does not need an additional definition.
The hydroelectric power plant model consists of a generator, a 2-winding transformer and a busbar in DIgSILENT. The generator used is a synchronous machine which has an apparent power rating of 150 MVA and a nominal voltage of 15.8 kV. It is operated at a power factor of 0.80 and has a YN connection type. The 2-winding step-up transformer has an apparent power of 200 MVA with HV of 132 kV and LV of 15.8 kV. The vector group of the transformer is a Dyn11.

IV. Simulation Process and Case Studies

This section of the paper discusses the simulations of the models and system network developed in sections II and III. The methodology designed is implemented here. The proposed South African network, and the designed BESS and PHS plant are simulated under different case studies. which are discussed in detail including the procedures in the simulation software that were used in the process. All the simulations were executed in DIgSILENT PowerFactory 2018 software.

A. Case 1: Network with Wind Power Generation

In this case study, firstly, a load flow analysis was performed with the inclusion of 14 wind farms at Substation A (Total wind generation output of 848 MW) and B (Total wind generation output of 649 MW) respectively. The purpose is to investigate how the network performs with a large amount of wind power generation under steady-state.

Secondly, the network was simulated under a three-phase fault. The purpose is to observe the impact of wind farms on the voltage stability of the system under fault conditions.

B. Case 2: Network with Wind Power Generation and BESS

In this case, firstly, a load flow is performed, where four BESS are placed at bus bars connected to the loads in the respective substations. The loads in this paper are considered as customers in remote areas in the Eastern Cape that rely on the peaking power system for power supply.

Secondly, the network was simulated under three-phase fault with BESS, with the primary function of improving the voltage stability during both steady-state and fault conditions.

C. Case 3: Network with Wind Power Generation and PHS

This case investigated the ability of a PHS plant to improve the substation load voltage levels under steady-state and fault conditions. Given the geographical limitations of PHS, it will only be connected to 'Sub B Bus 4'. This busbar supplies the load in Substation B, and it is connected to Line 2 BC which is the line that experiences the fault.

The capacity of the PHS is 120 MW which is equivalent to the sum of the BESS (i.e. each BESS model is rated at 30 MVA) implemented in Case 3. The load flow was then performed on the network with PHS. Secondly, the network was simulated under a three-phase fault.

V. Results and Discussions

In this chapter, the results obtained from the cases studied in Chapter 4 above are outlined and discussed in detail. Firstly, the load flow results under steady-state conditions are tabulated and analyzed in A. Thereafter, only three-phase fault conditions are discussed from B till D. The voltage levels of the network will be checked if they lie within the acceptable voltage limits of 0.95 p.u. and 1.05 p.u. as required by [10].

A. Case 1: Network Steady-state Operation

As mentioned, in section III, the small-scale network was simulated in DIgSILENT PowerFactory under steady-state conditions for Case 1, Case 2 and Case 3. After three successful iterations the following voltage magnitudes shown in Table 1 were obtained:

TABLE 1: VOLTAGE MAGNITUDES UNDER STEADY-STATE OPERATION

	Voltage Magnitude in p.u.		
	With Wind	With BESS	With PHS
Load 1	0.976	0.993	0.975
Load 2	0.953	0.997	0.953
Load 3	0.968	0.991	0.969
Load 4	0.970	0.992	0.971

In Table 1, Load 1 and 2 are two loads located at Substation A and their voltage magnitudes lie within the acceptable voltage limit.

When the BESS is introduced into the network with wind power generation, the voltage magnitudes for Load 1 and Load 2 increased from 0.976 p.u. and 0.953 p.u. to 0.993 p.u. and 0.997 p.u. respectively. Load 3 is a load located at Substation B, while Load 4 is a load located at Substation C. Both of their voltage magnitudes lie within the acceptable range across all four cases. When the BESS is introduced into the network with wind power generation, the voltage magnitudes for Loads 3 and 4 increased from 0.968 p.u. and 0.970 p.u. to 0.991 p.u. and 0.992 respectively.

When PHS was introduced, the voltage levels remained relatively the same as the cases where there is an absence of any EES in the network. Therefore, when comparing the voltage levels through the use of BESS and PHS, it is evident that BESS has significantly improved the voltage levels of the loads under steady-state conditions.

B. Case 2: Fault Condition Operation Comparison with and without BESS

Four BESS in total were added in Substation A, B and C respectively. The external grids and substation load voltage levels are shown in Fig.6:
In Fig. 6 the voltage magnitudes for Load 1 and 4 have increased to 0.99 p.u., while that of Load 2 increased to 1 p.u. and Load 3 increased to 0.98 p.u. The substation load voltage magnitudes are all within the acceptable voltage limits. Thus, the inclusion of BESS has improved the voltage levels of the loads, which confirms the findings in the literature which state that BESS improves voltage stability.

Lastly, the voltage levels results obtained in Case 2 will now be compared to the results obtained in Case 3 to determine which EES will be most suitable to improve voltage levels for a small-scale network with a large amount of wind generation.

C. Case 3: Fault Condition Operation Comparison between Network with BESS and Network with PHS

A single PHS was connected to Substation B. The substation load voltage levels are shown in Fig. 7.

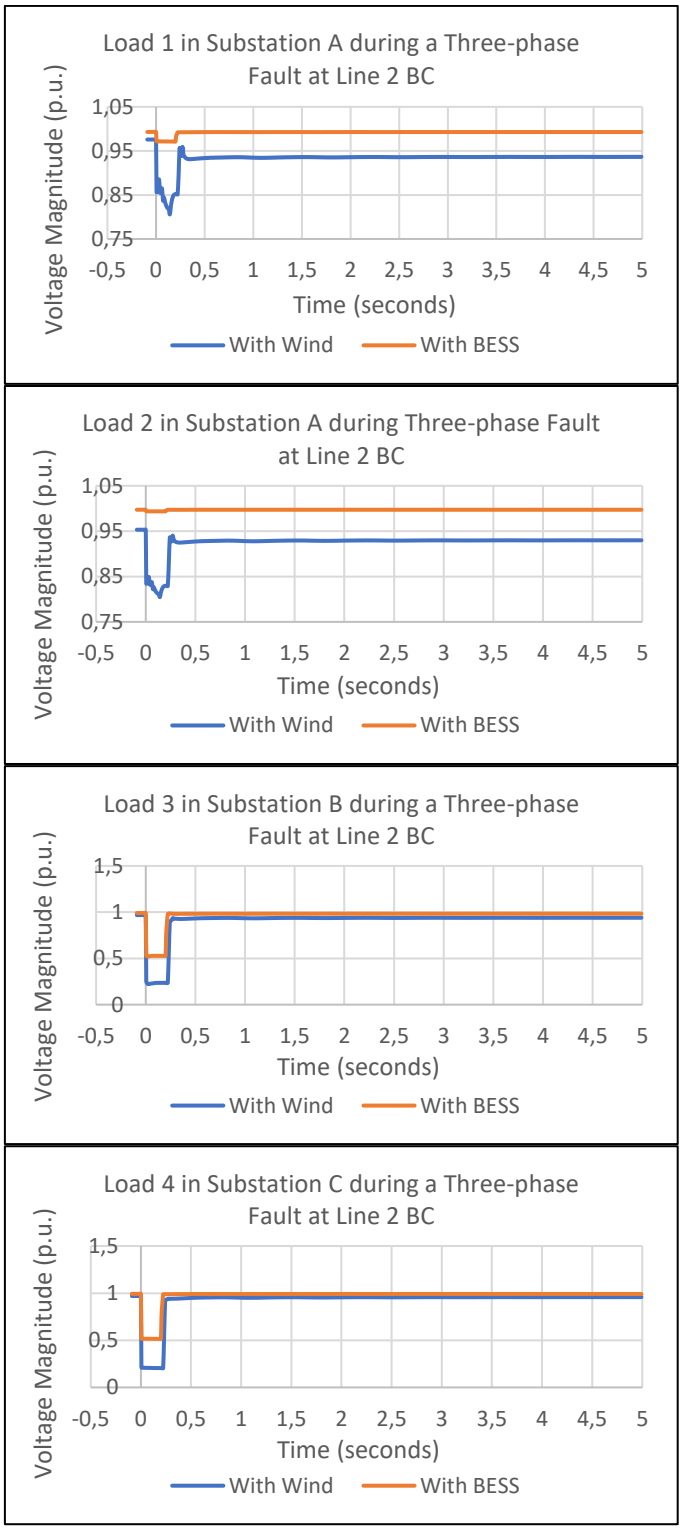

Fig. 6: Substation Loads Voltage Levels during a 3-Phase Fault with BESS

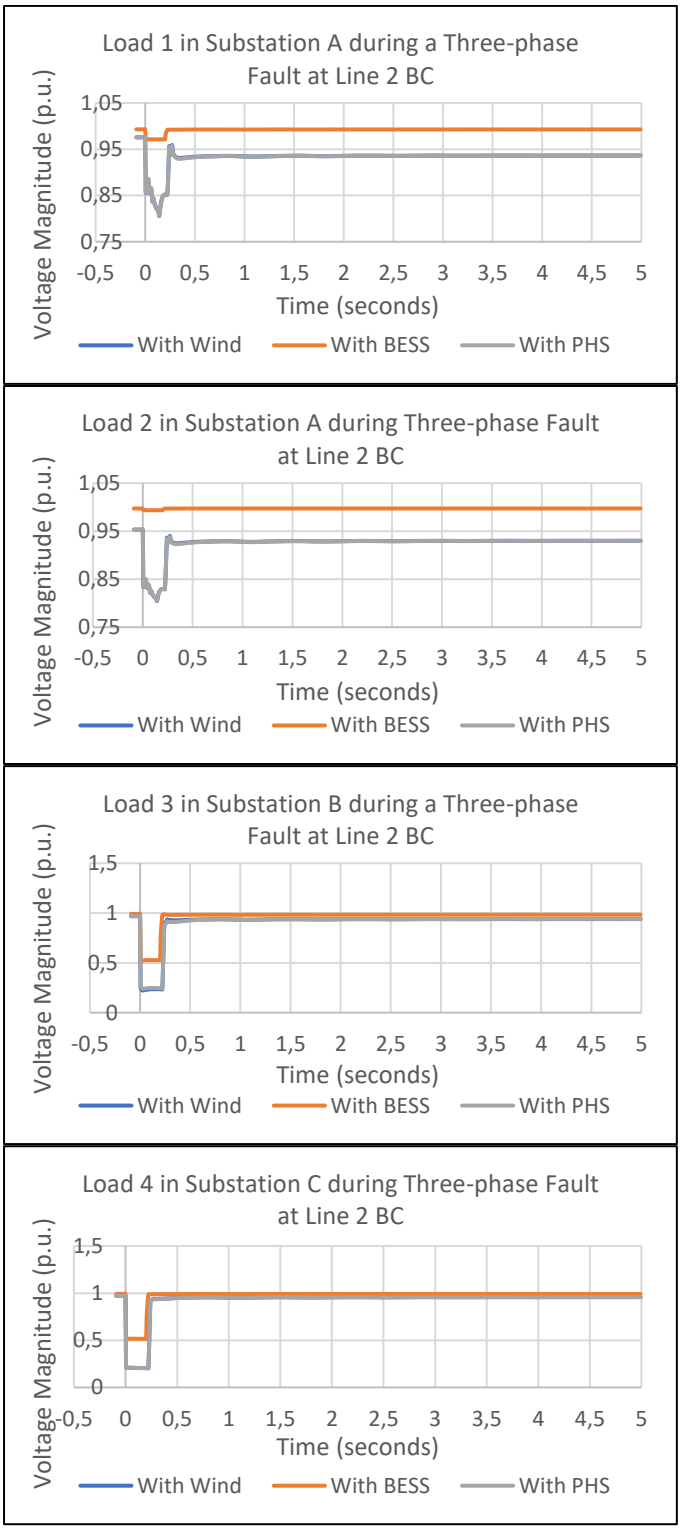

Fig. 7: Substation Load Voltage Levels during 3-Phase Fault with PHS Added

In Fig. 7 the voltage magnitudes for Load 1, 2 and 3 have decreased below the acceptable voltage limits. Load 1 and Load 3 both have voltage magnitudes of 0.94 p.u., which is significantly lower than 0.99 p.u. and 0.98 p.u. obtained in Case 2 respectively. Load 2 has the lowest voltage magnitude with 0.93 p.u. which is lower than the Load 2 voltage magnitude in

Case 3 of 1 p.u. Lastly, the voltage magnitude of Load 4 decreased to 0.96 p.u. from 0.99 p.u. in Case 2, but remains within the acceptable voltage range of 0.95 p.u. and 1.05 p.u. On the contrary, the voltage magnitudes of Load 1, 2 and 3 are below 0.95 p.u., while the voltage magnitudes with BESS all lie within the acceptable range.

VI. Conclusion

Under steady-state conditions, the voltage levels for the four loads lay within the acceptable voltage limits across all four cases. When the BESS was introduced into the network, the voltage magnitudes for the loads improved significantly, while the introduction of PHS led to voltage magnitudes of the loads remaining relatively the same as in cases where there was an absence of any EES in the network. Therefore, when comparing the voltage levels through the use of BESS and PHS, it is evident that BESS has significantly improved the voltage levels of the loads under steady-state conditions.

Under three-phase fault conditions with BESS, the voltage levels of the four loads lie within the acceptable voltage limits after the fault was cleared by opening the circuit breakers of Line 2 BC. While for the network only with wind generation or PHS the voltages for Load 1, 2 and 3 lie below the acceptable voltage limit.

Therefore, it can be concluded that BESS is the most suitable EES for a network with large amounts of wind generation, as it displayed the capability of maintaining the voltage levels within the acceptable voltage limits under both steady-state and fault conditions. Most importantly it improved other performance aspects of the network such as reducing oscillations after three-phase faults and providing active and reactive power support under steady-state conditions.

References

[1] Integrated Resource Plan 2018", *Energy.gov.za*, 2018. [Online]. Available: http://www.energy.gov.za/IRP/irp-update-draft-report2018/IRP-Update-2018-Draft-for-Comments.pdf. [Accessed: 28- Jul- 2019].

[2] H. Ibrahim, et al., "Integration of Wind Energy into Electricity Systems: Technical Challenges and Actual Solutions", *Energy Procedia*, vol. 6, pp. 815-824, 2011.

[3] D. O. Akinyele and R. K. Rayudu, "Review of energy storage technologies for sustainable power networks," *Sustain. Energy Technol. Assessments*, vol. 8, pp. 74–91, 2014.

[4] M. Ceraolo, "New Dynamical Models of Lead-Acid Batteries," *IEEE Transmission Power Systems*, vol. 15, no. 4, pp. 1184-1190, 2000.

[5] L. Festinger, "Development of Differential Appetite in the Rat," *J. Exp. Psychol.*, vol. 32, no. 3, pp. 226-234, 1943

[6] "Battery Energy Storage Systems", *Digsilent.de*, 2010. [Online]. Available: https://www.digsilent.de/en/faq-reader-powerfactory/do-you-have-an-application-example-for-a-battery-energy-storage-system-bess/tags/battery.html. [Accessed: 03- Sep- 2019].

[7] N. Tephiruk, et al. "Fuzzy Logic Control of a Battery Energy Storage System for Stability Improvement in an Islanded Microgrid," *Sustainability*, vol. 10, no. 5, pp. 1645, 2018.

[8] J. Stanojevic, A. Djordjevic, and M. Mitrovic, "Influence of Battery Energy Storage System on Generation Adequacy and System Stability in Hybrid Microgrids," *4th Int. Symp. Environ. Friendly Energies Appl. EFEA 2016*,

[9] K. Papadopoulos, "DIgSILENT PowerFactory Application Guide Dynamic Modelling Tutorial DIgSILENT Technical Documentation," Academia.edu, 2013. [Online]. Available: https://www.academia.edu/33570936/DIgSILENT_PowerFactory_Application_Guide_Dynamic_Modelling_Tutorial_DIgSILENT_Technical_Documentation. [Accessed: 23-Sep-2019].

[10] "ELECTRICITY SUPPLY — QUALITY OF SUPPLY Part 2: Voltage characteristics, compatibility levels, limits and assessment methods", *Nersa.org.za*, 2010. [Online]. Available: http://www.nersa.org.za/Admin/Document/Editor/file/Electricity/IndustryStandards/NRS048%20part%202.pdf. [Accessed: 30- Sep- 2019]